

# Interrupted chain assisted Al atomic wires on Si(211)

Bikash C Gupta and Inder P. Batra

Department of Physics, 845 W Taylor street, University of Illinois at Chicago, Chicago, Illinois 60607-7059, USA

(Dated: November 20, 2018)

Possibility for the formation of stable Al atomic wire on the Si(211) surface is investigated using density functional theory based total energy calculations. The stable adsorption sites and the surface structures at various sub-monolayer coverages of Al are presented. It is found that the most stable and natural surface structures around one monolayer coverage is either  $1 \times 5$  or  $1 \times 6$  which agrees with experimental observations. More significantly, our study revealed that unlike the case of Ga the formation of continuous atomic Al chains assisted by interrupted Al chains may be possible by controlling the experimental conditions (pressure and temperature) such that the  $\mu_{\text{Al}}$  remains within  $\sim 0.3$  eV from the bulk value. While the Al covered Si(211) surface may be metallic or semiconducting, the Ga covered Si(211) is always semiconducting in nature below 1 ML coverage. Also significant is the fact that Al atoms move from groove sites to the sites between terrace and trench atoms through lower energy channels as the coverage goes from  $1/8$  monolayer to  $1/4$  monolayer.

PACS numbers: 73.20.-r, 73.21.Hb, 73.90.+f

## I. INTRODUCTION

Technological importance of nanowire structures on silicon substrates has generated much interest in studying structural arrangements of metals on various Si substrates.<sup>1,2</sup> In particular, metals like Al, Ga and In at sub-monolayer coverages on the Si(001) surface have been examined<sup>3,4</sup> for the formation of stable atomic wires on surfaces. Though, stable atomic wire structures have not been found on the bare Si(001) surface, there has been some progress<sup>5,6,7</sup> towards the formation of stable atomic wires on the patterned hydrogen terminated Si(001) surface.

Recently, the vicinal Si surfaces have attracted much attention for the growth of self assembled atomic wires on them. The Si(211) surface<sup>8,9</sup> is one of the vicinal Si surfaces that is being widely used by experimentalists<sup>10,11,12,13</sup> as a substrate for growing atomic wire structures. This surface can be viewed as a stepped arrangement of narrow (111) terraces.

A three dimensional view of a small portion of the ideal Si(211) surface is shown in Fig. 1. The atoms marked T (called the terrace atoms) on the terrace are three-fold coordinated and thus have one dangling bond each; those on the step edge, marked E (called the edge atoms) are two-fold coordinated and have two dangling bonds each. Second layer Si atoms which are not directly bonded either with terrace or edge atoms are denoted as Tr (called the trench atoms) have one dangling bond each. The Si(211) surface consists of two-atom wide terraces between terrace and edge atoms along the  $[\bar{1}11]$  direction. Two consecutive terraces are separated by steps and are  $9.4 \text{ \AA}$  apart in the  $[\bar{1}11]$  direction, while they extend infinitely along  $[01\bar{1}]$ . The reason for using Si(211) is that the metals are expected to nucleate at the step edges, and form atomic nanowires.

The scanning tunneling microscopy (STM) images obtained by Baski et al.<sup>12</sup> for the Ga/Si(211) system showed

the formation of atomic wires of Ga extending along the  $[01\bar{1}]$  direction with vacancies at every fifth or sixth atoms interval *i.e.*, the surface structure becomes  $1 \times N$  with  $N=5-6$ . The Ga wires were separated by  $9.4 \text{ \AA}$  along the  $[\bar{1}11]$  direction. These authors also provided a theoretical model supporting their experimental observations. The same system was also studied by Gonzalez et al.<sup>13</sup> and their STM images revealed the formation of two atomic chains of Ga extending along the  $[01\bar{1}]$  direction within the  $9.4 \text{ \AA}$  distance along the  $[\bar{1}11]$  direction. They also found that both the chains have vacancies at six atoms interval along the  $[01\bar{1}]$  direction *i.e.*, the surface structure is  $1 \times 6$ . The authors, in addition, performed a detailed theoretical calculations in support of their experimental results. From the experimental and theoretical results for Ga/Si(211), it is clear that a stable uninterrupted Ga chain can not be formed on the Si(211) substrate. The In/Si(211) system has also been studied experimentally by means of STM, low energy electron diffraction (LEED) and Auger electron spectroscopy (AES). It is found that the surface pattern is  $1 \times 7$ .<sup>14</sup> They also presented an intuitive model in support of their results. Wang et al.<sup>15</sup> performed LEED experiments on the Al/Si(211) at sub-monolayer coverage and they found the surface pattern to be  $1 \times 6$ . The question we raise here is whether or not a stable uninterrupted atomic Al chain may be formed on the Si(211) substrate. Since, no detailed electronic structure calculations have so far been made for the precise atomic arrangements of Al on the Si(211) surface, the possibility of formation of a stable continuous Al wire on Si(211) is also worth investigating. In this paper we therefore perform extensive total energy calculations for the Al/Si(211) system.

From theoretical perspective it is important to know the reconstruction of the clean surface prior to the placement of any metal on the surface. As far as the reconstruction of the clean Si(211) surface is concerned, there have been several studies<sup>15,16,17,18</sup>. However, Baski et

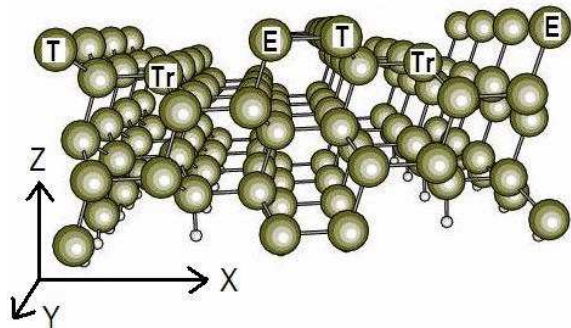


FIG. 1: Atoms in perspective form the ideal Si(211)  $2 \times 4$  super-cell. The bottom layer Si atoms are passivated by hydrogen atoms (small circles). Surface terrace, trench and edge atoms are denoted as T, Tr and E respectively. X, Y and Z directions correspond to  $[\bar{1}11]$ ,  $[0\bar{1}\bar{1}]$  and  $[211]$  respectively

al.<sup>19</sup> found (using STM) that the clean Si(211) is really unstable and consists of nanofacets with (111) and (337) orientations. It has also been shown that the Si(211) orientation is regained upon metal adsorption.<sup>12,13</sup> In view of this result,<sup>12,13</sup> we therefore consider the ideal bulk terminated Si(211) substrate for the Al atomic wires study. In our investigations, we systematically increase Al coverage on the Si(211) surface and see how the adsorption sites and the surface structure change as we go towards a monolayer (ML) coverage. We will show that atomic arrangement of Al on Si(211) will depend on the chemical potential of Al ( $\mu_{Al}$ ) which in turn depends on the experimental conditions such as the substrate temperature, the Al vapor pressure in the effusion cell and the Al vapor pressure on the substrate. Our study reveals that the interrupted Al chains with period five/six (similar to the case of Ga) may be formed. However, most significant result in this investigation is that a stable uninterrupted Al chain extending along the  $[0\bar{1}\bar{1}]$  direction assisted by an interrupted chain can be formed at about 1 ML coverage.

The paper is organized as follows. In Section II we present the parameters used in the pseudopotential density functional calculations. The results and discussions are presented in Section III. Finally, in section IV, we summarize our principal findings.

## II. METHOD

Total energy minimization calculations are carried out within the density functional theory (DFT) in conjunction with the pseudopotential approximation. The Si(211) surface is represented in a repeated slab geometry. Each slab contains seven Si(211) layers with a vacuum region of 12 Å. For example, in the  $1 \times 4$  super-cell, each layer contains eight Si atoms: two along  $[\bar{1}11]$  and four along  $[0\bar{1}\bar{1}]$ . The top layer (within the  $1 \times 4$  super-cell) contains four edge and four terrace Si atoms. It is noted that in an ideal Si(211): $1 \times 1$  surface each layer

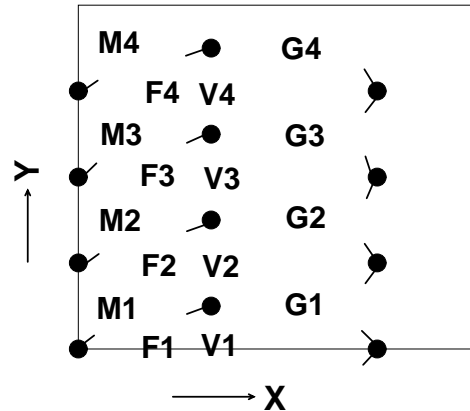


FIG. 2: Filled circles represent Si atoms of the bulk terminated Si(211) surface within a  $1 \times 4$  supercell. First, second, and third column of atoms are terrace, trench and edge atoms respectively. Dangling bonds of all the atoms are shown. Various kinds of symmetric sites are designated as G, V, F, and M sites respectively. The numerals 1, 2, 3, and 4 indicate identical sites displaced along the Y direction in the super-cell. For example, G1, G2, G3 and G4 (Groove sites) are identical sites displaced by 3.84 Å along the Y direction in the super-cell.

consists of two distinct atoms. The Si atoms in the bottom layers have their dangling bonds saturated by hydrogen atoms (see Fig. 1). Since the edge atoms have two dangling bonds each, the trench atoms have one dangling bond each and the terrace atoms have one dangling bond each, we require sixteen hydrogen atoms to saturate all the dangling bonds at the bottom of the slab in the  $1 \times 4$  super-cell. We have used super-cells of various sizes ( $1 \times 2$ ,  $1 \times 3$ ,  $1 \times 4$ ,  $1 \times 5$ ,  $1 \times 6$ , and  $1 \times 7$ ) in our calculations. The top five Si layers are relaxed for geometry optimization while the two lower-most Si layers and the hydrogen atoms are held fixed to simulate the bulk-like termination. The wave functions are expanded in a plane wave basis set with a cutoff energy  $|\vec{k} + \vec{G}|^2 \leq 250$  eV. The Brillouin zone (BZ) integration is performed within a Monkhorst-Pack (MP)<sup>20</sup> scheme using four inequivalent k-points. It has been established earlier<sup>17</sup> that the energy cutoff, the set of k-points, the number of layers in the slab and the amount of vacuum region considered here give sufficiently converged values for total energies. Ionic potentials are represented by Vanderbilt-type ultra-soft pseudopotentials<sup>21</sup> and results are obtained using generalized gradient approximation (GGA)<sup>22</sup> for the exchange-correlation potential. Preconditioned conjugate gradient is used for wave function optimization and a conjugate gradient for ionic relaxations. The Z axis is taken perpendicular to the Si(211) surface, while X and Y axis are along  $[\bar{1}11]$  and  $[0\bar{1}\bar{1}]$  respectively. The VASP code<sup>23</sup> is used for our calculations.

### III. RESULTS AND DISCUSSIONS

The structures and energetics for Al on the Si(211) surface at 1/8, 1/4, 1/2 and beyond 1/2 ML coverages are systematically analyzed here to examine the formation of Al atomic wires on the Si(211) substrate. Note that one monolayer corresponds to one atom per Si atom on the top layer of the ideal bulk terminated surface leading to  $\sim 5.56 \times 10^{14}$  atoms/cm<sup>2</sup>.

#### A. Structure and energetics of Al at 1/8 ML coverage on Si(211)

Here we discuss the structure and energetics of Al at 1/8 ML coverage and hence we need to place one Al atom on the surface of  $1 \times 4$  super-cell. At such a low coverage the Al atoms are practically isolated from each other on the surface. The Si(211) surface offers various kinds of sites for Al to bind. Based on the symmetry and available dangling bonds on the surface, we consider all the probable binding sites which are designated as G, V, M, and F sites respectively in Fig. 2. We use numerals 1, 2, 3 and 4 to label identical sites displaced by 3.84 Å along the  $[01\bar{1}]$  direction in the super-cell. For example, G1, G2, G3 and G4 (G sites) are identical sites displaced by 3.84 Å along the  $[01\bar{1}]$  direction in the super-cell. The binding energies (BE) of the Al atom at different kinds of sites are given in Table I. The binding energy of the Al atom is defined as  $BE = -[E(\text{Al} + \text{Si}) - E(\text{Si}) - E_{\text{Al}}]$  where  $E(\text{Al} + \text{Si})$ ,  $E(\text{Si})$  and  $E_{\text{Al}}$  are total energy of Al adsorbed super-cell, total energy of the super-cell without Al and atomic energy of Al respectively.

From Table I, we notice that a G site (BE=4.53 eV) is most favorable for Al adsorption followed by a F site (BE=4.45 eV), and a V site (BE=4.31 eV) respectively. Binding energy of Al at a V site is close to that at a M site. In our calculations, we let the Al atom (except at V sites) relax in all directions so as to reach the local energy minimum. For V site, the Al atom is allowed to relax both along Y and Z directions. It is reasonable that the Al atom favors to bind at a site where it can satisfy itself by sharing charges with three neighboring Si atoms. At a G site the Al atom is surrounded by two edge Si atoms and one trench Si atom. The distance of the Al atom (at a G site) from the nearest edge Si atoms are  $\sim 2.6$  Å and that from the nearest trench Si atom is also  $\sim 2.6$  Å. On the other hand, the Al atom at the F site also shares its charge with three Si neighbors and the Al-Si bonds at those sites are equally strong as that at a G site. For example, the distances of the Al atom at a F site from its neighboring terrace and two trench Si atoms are 2.6 Å, 2.5 Å and 2.5 Å respectively. Furthermore, the charge density plot in Fig. 3 clearly shows that the Al atom at both the G and F sites makes strong bonds with three neighboring Si atoms. We also notice that the edge Si atoms form dimers irrespective of the position of the Al atom at a G site or a F site. However, as the Al atom

TABLE I: Binding energies (BE) for Al at G1, F1, V1 and M1 sites on the bulk terminated Si(211) at 1/8 ML coverage.

Site:	G1	F1	V1	M1
BE (eV):	4.52	4.45	4.31	4.30

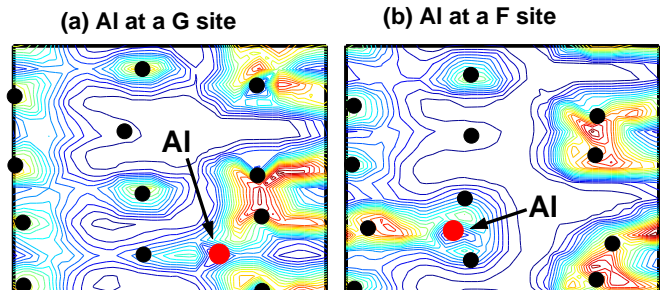


FIG. 3: Total charge distribution on a plane just above the top Si layer at 1/8 ML coverage: (a) when the Al atom is placed at a G site and (b) when the Al atom is placed at a F site. In both figures, circles in the first, second and third columns are terrace, trench and edge Si atoms respectively while the Al atoms are indicated by arrows.

forms bonds with the neighboring Si atoms, it introduces strain in the underlying lattice. Therefore the net energy gain due to Al adsorption will also depend on the amount of strain introduced by the Al atom during the process of forming bonds with the neighboring Si atoms. From Fig. 3(b) it is evident that one of the edge Si dimers in the super-cell is distorted due to the strain introduced by the Al atom adsorbed at a F site. As a whole, a G site turns out to be most favorable. The net energy gain in this process is the difference between the binding energy of Al at a G site and its chemical potential,  $\Delta E = (BE - |\mu_{\text{Al}}|) \sim 0.85$  eV, where  $\mu_{\text{Al}} = -3.68$  eV is the bulk chemical potential for aluminum. However, in practice, the energy gain will be less than 0.85 eV as the bulk chemical potential is the upper bound of  $\mu_{\text{Al}}$ . In other words, a maximum of  $\sim 0.85$  eV is gained by adsorbing an Al atom at a G site.

Our calculations show that the adsorption of Al atom on the terrace site is not possible because one needs to supply an energy of  $\sim 1$  eV to place an Al atom on the terrace Si atom. We also studied the energetics for the replacement of terrace, trench and edge Si atoms by Al atoms. Our results indicate that replacement of trench and edge Si atoms by Al atoms are energetically not possible, while an energy of 0.5 eV is gained due to the replacement of a single terrace Si atom by an Al atom. We note that the chemical potential for Si ( $\mu_{\text{Si}}$ ) is taken to be the bulk value  $\sim -5.43$  eV. This information will be useful in the later part of our discussion at higher coverages of Al.

### B. Structure and energetics of Al at 1/4 ML coverage on Si(211)

To analyze the structure and energetics of Al on Si(211) at 1/4 ML coverage we place two Al atoms on the bulk terminated Si(211) surface of the  $1 \times 4$  super-cell. Based on the results at 1/8 ML coverage and on physical grounds, we consider various reasonable combinations of a couple of sites where Al atoms may prefer to bind. The composite sites that we consider are G1G3 (one Al atom is placed at G1 site and the other is placed at G3 site on the surface of the  $1 \times 4$  super-cell), G1F3 (one Al atom is placed at G1 site and the other is placed at F3 site), G1M3 (one Al atom is placed at G1 site and the other is placed at M3 site), F1F3 (one atom is placed at F1 site and the other is placed at F3 site) and M1M3 (one atom is placed at M1 site and the other is placed at M3 site) respectively. Without doing any calculations and just based on the results at 1/8 ML coverage, one may conclude that the composite site, G1G3 should be preferable for Al. However, in the presence of two Al atoms the surface may undergo further reconstructions due to the interaction with the surface Si atoms and hence, G1G3 may not be the most favorable composite site. We therefore, perform extensive calculations for Al adsorption at all the composite sites. The average binding energies per Al atom are given in Table II. By examining Table II, it turns out that G1G3 configuration is the least favorable (BE per Al is  $\sim 4.2$  eV) configuration while the most favorable configuration is M1M3 (BE per Al is  $\sim 4.4$  eV).

We note that while M sites turned out to be least favorable among the G, F, V and M sites at 1/8 ML coverage, it becomes most favorable at 1/4 ML coverage. In other words, the Al atoms move from the G sites to M sites through lower energy channels (with a barrier height of  $\sim 0.3$  eV) as the coverage goes from 1/8 ML to 1/4 ML. The strain induced in the underlying lattice due to the adsorption of Al atoms are responsible for such happenings. At 1/4 ML coverage, the surface consists of Al chains lying between terrace and trench atoms and extending along the  $[0\bar{1}1]$  direction with an interatomic distance of 7.68 Å. Therefore the preferable binding sites for Al and hence the arrangement of surface atoms are highly coverage dependent.

The total charge distribution on a plane just below the Al layer for M1M3 and G1G3 configurations are shown in Fig. 4. We observe that the Al atoms in both the configurations form strong bonds with their neighboring Si atoms. We however note that while the edge Si atoms in the M1M3 configuration form strong dimers (dimer length  $\sim 2.3$  Å) to reduce the total energy of the system, they are unable to form strong dimers (dimer length  $\sim 2.9$  Å) in the G1G3 configuration due to the strain induced by the Al atoms. This is one of the reasons for favoring M1M3 configuration over the G1G3 configuration. At this 1/4 ML Al coverage, the average binding energy per Al atom is slightly lower (by 0.1 eV) than that at 1/8 ML coverage. We conclude that at 1/4 ML coverage of

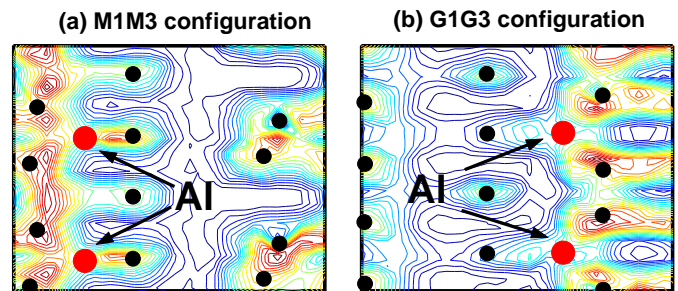


FIG. 4: The total charge distribution on a plane just below the Al layer at 1/4 ML coverage of Al on Si(211): (a) the most favorable configuration, M1M3 and (b) the G1G3 configuration. Al atoms are indicated by arrows. The small circles represent the terrace, trench and edge atoms respectively as one goes from left to right column.

TABLE II: Average Binding energy (BE) per Al atom at 1/4 ML coverage. A set of two sites combinations on the bulk terminated Si(211) are considered and they are denoted as G1G3, G1F3, G1M3, F1F3 and M1M3 respectively.

Site:	G1G3	G1F3	G1M3	F1F3	M1M3
BE (eV):	4.22	4.26	4.33	4.37	4.43

Al the surface structure symmetry becomes  $1 \times 2$  and the maximum energy gain per Al atom in the process of adsorbing two Al atoms at the M1 and M3 sites on the surface of the  $1 \times 4$  super-cell is  $\sim 0.75$  eV.

### C. Structure and energetics of Al at 1/2 ML coverage on Si(211)

The Al coverage is now increased to 1/2 ML *i.e.*, four Al atoms are placed on the surface of the  $1 \times 4$  super-cell. Based on previous results at low coverages and the dangling bonds available on the surface we consider three plausible combinations of four sites on the surface. They are designated as M1M2M3M4 (four Al atoms are placed at M1, M2, M3 and M4 sites available on the surface of the super-cell), G1G3M2M4 (four Al atoms are placed at G1, G3, M2 and M4 sites available on the surface of the super-cell) and G1G2G3G4 (four Al atoms are placed at G1, G2, G3 and G4 sites available on the surface of the super-cell) respectively. The average binding energy per Al atom for all the configurations are given in Table III. We note that average energy gain per Al atom for the configurations G1G3M2M4 (BE  $\sim 4.3$  eV) and G1G2G3G4 (BE  $\sim 4.4$  eV) are very close to each other. The charge density plot for the G1G3M2M4 configuration is shown in Fig. 5(a). We note from Fig. 5(a) that all the four Al atoms make bonds with their neighboring Si atoms and the edge Si atoms form dimers. All the Al atoms remain more or less on the same plane and saturates all the surface dangling bonds. Therefore, for the

TABLE III: Average Binding energy (BE) per Al atom at 1/2 ML coverage. A set of four sites combinations on the bulk terminated Si(211) are considered and they are denoted as M1M2M3M4, G1G3M2M4 and G1G2G3G4 respectively.

Site:	M1M2M3M4	G1G3M2M4	G1G2G3G4
BE (eV):	3.88	4.30	4.37

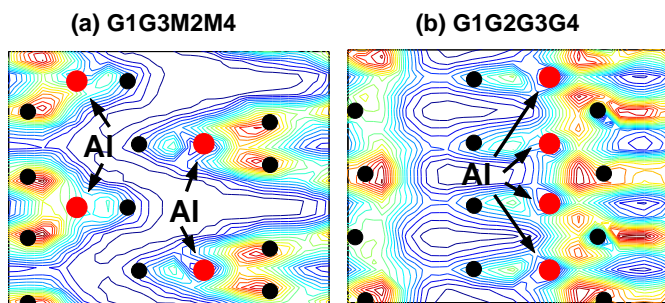


FIG. 5: The charge distribution just below the Al layer at 1/2 ML coverage of Al on Si(211): (a) second best favorable configuration, G1G3M2M4 and (b) the most favorable configuration, G1G2G3G4. Al atoms are indicated by arrows in the figures.

G1G3M2M4 configuration, the highly terraced Si(211) surface becomes more or less flat decorated by parallel zigzag Al chains separated by 9.4 Å and extending along the  $[01\bar{1}]$  direction. However, for the most favorable configuration, G1G2G3G4, the terrace Si atoms remain unsaturated, all the Al atoms remain on the same plane and make strong bonds with the neighboring trench and edge Si atoms. Thus, at 1/2 ML Al coverage, the Si(211) surface becomes a flat surface decorated with straight parallel Al chains separated by 9.4 Å and running along the  $[01\bar{1}]$  direction (see charge density plot in Fig. 5(b)). The average energy gain per Al atom in the process of bringing four Al atoms from the source and putting them at G1,G2,G3, and G4 sites is 0.7 eV which is substantial. A comparison of the configurations G1G3M2M4 and G1G2G3G4 suggests that the complete saturation of surface dangling bonds does not necessarily lead to the most favorable structure here and hence the surface strain induced by the adsorbed Al atoms becomes a significant factor for the most favorable structure. We therefore conclude that straight Al chains lying between the trench and edge Si atoms (*i.e.*, on the G sites) and extending along the  $[01\bar{1}]$  direction can be formed. We find that the binding energy per Al atom decreases with increasing coverage.

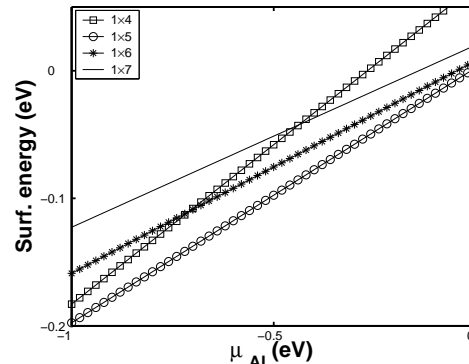


FIG. 6: The surface energies (eV) for Al chains having vacancies with period four ( $1 \times 4$ ), five ( $1 \times 5$ ), six ( $1 \times 6$ ) and seven ( $1 \times 7$ ) relative to the no vacancy case are plotted as a function of  $\mu_{\text{Al}}$ . Here the surface energy per  $1 \times 1$  super-cell surface area ( $\sim 36.11 \times 10^{-16} \text{cm}^2$ ) is considered for comparison among chains with different vacancy periods. Note that the chemical potential of Al is given with respect to the chemical potential of bulk Al.

#### D. Structure and energetics of Al beyond 1/2 ML coverage on Si(211)

The formation of Al chain at 1/2 ML coverage is possible under ideal conditions because in experiments it is difficult to restrict the coverage at a predetermined fixed value. Therefore we want to examine the evolution of surface structure when the Al coverage is just below 1/2 ML and also when it is somewhat larger, tending towards 1 ML. A continuous chain lying between the trench and edge sites produces strain in the system which may be relieved by forming vacancies along the chain (like Ga<sup>12,13,24</sup>). We therefore compare the surface energies corresponding to interrupted Al chains as a function of the chemical potential of Al. Figure 6 shows the variation of surface energy as a function of  $\mu_{\text{Al}}$  for interrupted Al chains (lying on the G sites) with different vacancy periods. The solid line with squares correspond to the surface energy for the formation of an Al chain that is interrupted at every fourth site and resulting surface pattern becomes  $1 \times 4$ . Similarly the solid lines with circles ( $1 \times 5$ ), stars ( $1 \times 6$ ) and the solid line with no symbol ( $1 \times 7$ ) correspond to Al chains with vacancy periods 5,6 and 7 respectively. The surface energies are plotted relative to the surface energy for the continuous chain (chain without vacancy). We note that the surface energies for  $1 \times 2$  and  $1 \times 3$  surface structures are not plotted here because they are very large compared to those shown in Fig. 6. We know that the upper limit of  $\mu_{\text{Al}}$  is the bulk chemical potential of Al ( $\mu_{\text{Al}}^{\text{Bulk}}$ ) which is taken as the reference in the figure. However, the practical value of  $\mu_{\text{Al}}$  depends on the experimental conditions. The thermodynamic relation between the  $\mu_{\text{Al}}^{\text{Bulk}}$  and the practical value of  $\mu_{\text{Al}}$  is given by the relation<sup>13</sup>

$$\mu_{\text{Al}} = \mu_{\text{Al}}^{\text{Bulk}} - k_B T \ln(p_c/p_s) \quad (1)$$

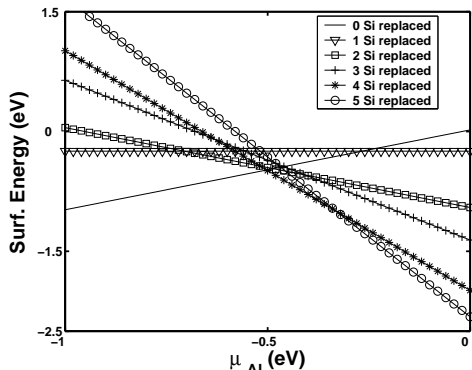


FIG. 7: The surface energies (eV) as a function of  $\mu_{\text{Al}}$  for the situations where zero (solid line), one (solid line with inverted triangles), two (solid line with squares), three (solid line with plus signs), four (solid line with stars) and five (solid line with circles) terrace Si atoms are replaced (in the  $1 \times 5$  supercell) by Al atoms respectively in the presence of an interrupted Al chain with vacancy period five on the groove sites. Surface energies relative to that for the no vacancy case is plotted. Note that the chemical potential of Al is given with respect to the chemical potential of bulk Al.

where  $p_c$  is the Al vapor pressure in the effusion cell and  $p_s$  is the Al vapor pressure at the sample and  $T$  is the sample temperature. Therefore,  $\mu_{\text{Al}}$  is always less than  $\mu_{\text{Al}}^{\text{Bulk}}$ . Experimental conditions can be set up to make this difference up to  $\sim 1$  eV. We observe from Fig. 6 that the interrupted chain with a vacancy period of five is energetically most favorable up to 1 eV below the  $\mu_{\text{Al}}^{\text{Bulk}}$ . However, in the range  $0.7 \text{ eV} < |\mu_{\text{Al}}| < 0 \text{ eV}$ , the next favorable chain is the one with six vacancy period. These interrupted Al chains with vacancy period five and six corresponds to an Al coverage slightly lower than  $1/2$  ML. However, to find the lowest surface energy structure we need to go beyond  $1/2$  ML coverage.

Therefore, we next consider the interrupted chain with vacancy period five and see how the surface energy changes if we add more Al atoms to the surface. Although the adsorption of Al atoms at the terrace sites is energetically not possible, terrace Si atoms may well be replaced by Al atoms. Figure 7 shows the variation of surface energies for replacement of zero, one, two, three, four and five terrace Si atoms by Al in the presence of an interrupted Al chain (on the groove sites with vacancy period five) as a function of  $\mu_{\text{Al}}$ . The solid lines with inverted triangle, square, plus sign, star, and circle symbols correspond to the situations where one, two, three, four and five terrace Si atoms are replaced by Al respectively in the presence of a  $1 \times 5$  interrupted chain. The solid line corresponds to the no replacement case. We clearly notice that there are three different regimes for  $\mu_{\text{Al}}$  favoring different Al configuration. (i) For,  $0 \text{ eV} < |\mu_{\text{Al}}| \lesssim 0.3 \text{ eV}$ , the replacement of all terrace Si atoms are favorable in the presence of a  $1 \times 5$  interrupted chain on the groove sites *i.e.*, the Si(211) surface will consist of one interrupted Al chain with vacancy period five on the groove

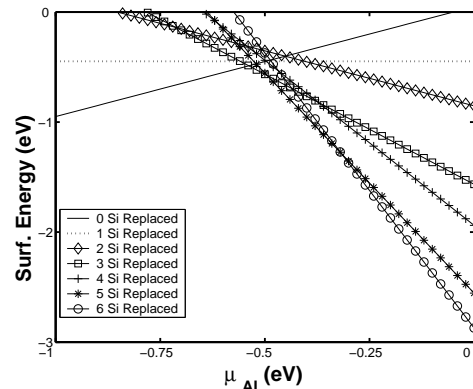


FIG. 8: The surface energies (eV) as a function of  $\mu_{\text{Al}}$  for the situations where zero (solid line), one (dotted line), two (solid line with diamonds), three (solid line with squares), four (solid line with plus signs), five (solid line with stars) and six (solid line with circles) terrace Si atoms are replaced (in the  $1 \times 6$  supercell) by Al atoms respectively in the presence of an interrupted Al chain with vacancy period six on the groove sites. Surface energies relative to that for the no vacancy case is plotted. Note that the chemical potential of Al is given with respect to the chemical potential of bulk Al.

sites along with a continuous Al chain on the terrace sites extending along the  $[01\bar{1}]$  direction (solid line with circles). (ii) For  $0.3 \text{ eV} < |\mu_{\text{Al}}| \lesssim 0.5 \text{ eV}$  the Si(211) surface favors an interrupted Al chain on the terrace sites with period five in the presence of the interrupted Al chain on the groove sites with a vacancy period five (solid line with stars). (iii) For  $|\mu_{\text{Al}}| \gtrsim 0.5$  the surface does favor any replacement of terrace Si atoms by Al atoms in the presence of the interrupted Al chain on the groove sites with a vacancy period five (*i.e.*, the surface consists of only interrupted Al chains with period five on the groove sites).

We already saw (in Fig. 6) that the interrupted Al chain on groove sites with the vacancy period six was the second most favorable structure in the practical regime of  $\mu_{\text{Al}}$ . It is therefore desirable to study the possibility of replacement of terrace Si atoms by Al atoms in the presence of  $1 \times 6$  interrupted chain also. Figure 8 shows the variation of surface energies for replacement of zero, one, two, three, four, five and six terrace Si atoms by Al in the presence of  $1 \times 6$  interrupted Al chain (on the groove sites) as a function of  $\mu_{\text{Al}}$ . The dotted line and the solid lines with diamond, square, plus, star, and circle symbols correspond to the situations where one, two, three, four, five and six terrace Si atoms are respectively replaced by Al atoms in the presence of  $1 \times 6$  vacancy chain on the groove sites. The solid line corresponds to the no replacement case. Similar to the Fig. 7 we again find in Fig. 8 that there are three different regimes for  $\mu_{\text{Al}}$  favoring different Al replacement/no-replacement configurations. (i) For,  $0 \text{ eV} < |\mu_{\text{Al}}| \lesssim 0.3 \text{ eV}$ , the replacement of all terrace Si atoms are favorable in the presence of  $1 \times 6$  vacancy chain on the groove sites *i.e.*, the Si(211) surface consists

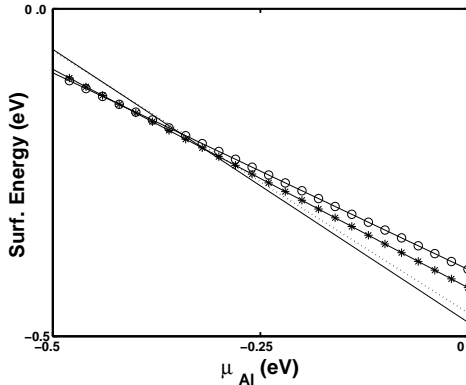


FIG. 9: The surface energies (eV) per  $1 \times 1$  super-cell surface area ( $\sim 36.11 \times 10^{-16} \text{ cm}^2$ ) as a function of  $\mu_{\text{Al}}$  for the following surface structures: (a) the uninterrupted Al chain on the terrace sites along with an interrupted chain on the groove sites with period five vacancy (dotted line), (b) the interrupted Al chain on terrace sites with period five vacancy along with an interrupted chain on the groove sites with period five vacancy (solid line with circles), (c) the uninterrupted Al chain on the terrace sites along with an interrupted chain on the groove sites with period six vacancy (solid line), and (d) the interrupted Al chain on terrace sites with period six vacancy along with an interrupted chain on the groove sites with period six vacancy (solid line with stars). Surface energies relative to that for the no vacancy case is plotted. Note that the chemical potential of Al is given with respect to the chemical potential of bulk Al.

of one interrupted Al chain with vacancy period six on the groove sites along with a continuous Al chain on the terrace sites extending along the  $[01\bar{1}]$  direction (solid line with circles). (ii) For  $0.3 \text{ eV} < |\mu_{\text{Al}}| \lesssim 0.5 \text{ eV}$  the Si(211) surface favors an interrupted Al chain on the terrace sites with period six in the presence of the interrupted Al chain on the groove sites with a vacancy period six (solid line with stars). However, (iii) for  $|\mu_{\text{Al}}| \gtrsim 0.5 \text{ eV}$  the surface does not favor any replacement of terrace Si atoms by Al atoms in the presence of the interrupted Al chain on the groove sites with a vacancy period six (solid line) *i.e.*, the surface consists of only interrupted Al chains with period six along the groove sites.

Comparing Figs. 6, 7, 8 we can conclude that for  $|\mu_{\text{Al}}| \geq 0.5 \text{ eV}$  the replacement of terrace Si atoms by Al is energetically unfavorable. The most favorable surface structure is  $1 \times 5$  where the surface consists of interrupted Al chains (with vacancy period five) lying between trench and edge Si atoms and extending along the  $[01\bar{1}]$  direction. When  $0 \text{ eV} < |\mu_{\text{Al}}| \lesssim 0.5 \text{ eV}$ , Figs. 7 and 8 suggest that the most probable surface structure around one ML Al coverage can be deduced by comparing the surface energies for four situations: (a) the uninterrupted Al chain on the terrace sites along with an interrupted chain on the groove sites with period five vacancy, (b) the interrupted Al chain on terrace sites with period five vacancy along with an interrupted chain on the groove sites with period five vacancy, (c) the uninterrupted Al chain on

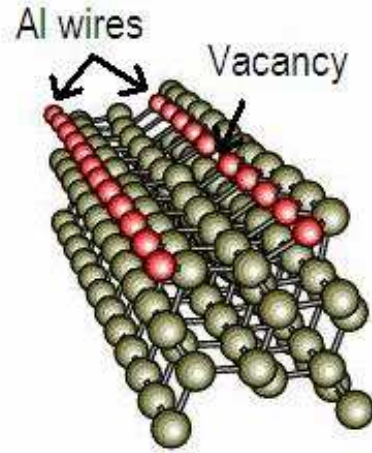


FIG. 10: The surface consists of two kinds of Al chains (indicated by arrows): one of them is uninterrupted and the other one is interrupted with a vacancy at a period of six. Both the chains are extending along the Y direction. This is the most favorable configuration for  $0 \text{ eV} < |\mu_{\text{Al}}| \lesssim 0.5 \text{ eV}$ .

the terrace sites along with an interrupted chain on the groove sites with period six vacancy, and (d) the interrupted Al chain on terrace sites with period six vacancy along with an interrupted chain on the groove sites with period six vacancy. These calculations present us with a rich set of possibilities for creating supported atomic wires on Si(211). Figure 9 shows the relative surface energies for such four surface structures in the range of  $|\mu_{\text{Al}}|$  between 0 and 0.5 eV. For  $0 \text{ eV} < |\mu_{\text{Al}}| \lesssim 0.3 \text{ eV}$  the surface structure corresponding to the solid line is most probable one ( $1 \times 6$ ) where the surface consists of two kinds of Al chains extending along the  $[01\bar{1}]$  direction: one is continuous and the other is interrupted with a vacancy period six (see Fig. 11). However, the surface energy represented by the dotted line is very close to that represented by the solid line and therefore the surface structure may also be  $1 \times 5$  where the surface consists of two kinds of Al chains extending along the  $[11\bar{1}]$  direction: one is continuous and the other is interrupted with a vacancy period five. In any case in the range,  $0 \text{ eV} < |\mu_{\text{Al}}| \lesssim 0.3 \text{ eV}$ , an interrupted Al chain with period five or six appears followed by a continuous Al chain. The interrupted chain, relieves the strain from the system to enable the formation of continuous Al chain. In this sense, the interrupted Al chain assists the formation of the continuous Al chain. In other words, in the range,  $0 \text{ eV} < |\mu_{\text{Al}}| \lesssim 0.3 \text{ eV}$ , continuous Al chains can be formed *assisted* by the interrupted Al chains with vacancy period five or six. It is worth recalling that the formation of continuous Ga chain is not possible on the Si(211) surface<sup>13</sup>. In the range of  $0.3 \text{ eV} < |\mu_{\text{Al}}| \lesssim 0.5 \text{ eV}$ , the surface energies for the solid lines with circles and stars (see Fig. 9) are lowest and they are very close to each other and hence we conclude that in this range

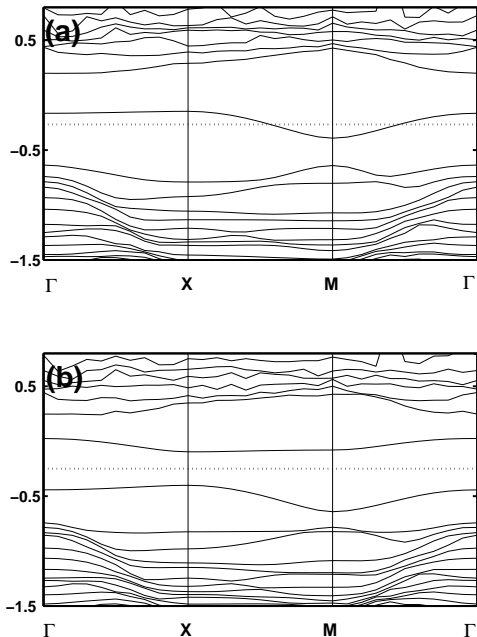


FIG. 11: Band structures: (a) for the surface consisting of continuous Al chains and interrupted Al chains with period  $1 \times 6$ ; (b) for the surface consisting of only interrupted Al chains with period  $1 \times 6$ . The dotted lines indicate the Fermi levels.

of  $\mu_{Al}$  uninterrupted Al chains will not be formed, *i.e.* the surface will consist of only interrupted chains and the surface structure will be either  $1 \times 5$  or  $1 \times 6$ . Since the surface structure and the arrangement of Al atoms on the Si(211) depends on  $\mu_{Al}$  which again depends on the experimental conditions, the observed surface structure upon Al deposition will depend on the experimental conditions. In other words, a desired surface structure among the many (discussed above) will be obtained by controlling the experimental condition. For example the uninterrupted Al chain assisted by interrupted Al chain may be formed if  $\mu_{Al}$  is typically maintained within the range of 0.3 eV from the bulk value. Our results indicate that the  $1 \times 6$  surface pattern of Al on the Si(211) observed by Wang et al.<sup>15</sup> is one of the most probable structures.

Band structures for two different surface structures are shown in Fig. 11. In Fig. 11(a), the band structure for the surface consisting of continuous Al chains and interrupted Al chains with period  $1 \times 6$  (most favorable surface structure for  $0 \text{ eV} < |\mu_{Al}| \lesssim 0.3 \text{ eV}$ ) reveals that the surface is metallic in nature. On the other hand, Fig. 11(b), indicates that the band structure for the surface consisting of only interrupted Al chains with period  $1 \times 6$  (one of the favorable structures for  $0.3 \text{ eV} < |\mu_{Al}| \lesssim 0.5 \text{ eV}$ ) is semiconducting in nature. We therefore conclude that below 1 ML Al coverage the Si(211) surface may be metallic or semiconducting in nature depending on the experimental conditions while the Ga covered Si(211) surface is only semiconducting in nature<sup>13</sup>. However, like

Ga/Si(211) an experimental study of Al/Si(211) is desirable.

#### IV. SUMMARY

Energy minimization calculations are performed to study the surface structures, due to adsorption of Al at various coverages on the Si(211) surface. Well below 1 ML coverage, we find that though the average binding energy per Al decreases slowly with increase of the coverage, the favorable sites change dramatically. For example at 1/8 ML coverage the Al atoms favors to bind at the groove (G) sites with an average binding energy  $\sim 4.52$  eV and at 1/4 ML coverage Al atoms prefers to bind at M sites with an average binding energy  $\sim 4.43$  eV. However, around 1/2 ML coverage Al atoms prefer to nucleate at the groove sites to form chain structure extending along the  $Y[01\bar{1}]$  direction with an interruption by a vacancy at regular intervals (with vacancy period 5 or 6). As the coverage increases further, the replacement process comes into play, *i.e.*, the terrace Si atoms are replaced by the Al atoms to form an uninterrupted/interrupted Al chain along the terrace sites in addition to the presence of the interrupted Al chain along the groove sites. A detailed analysis of our results reveals that for  $|\mu_{Al}| > 0.5$  eV, only interrupted Al chain along the groove sites with a vacancy period of five will be formed and for  $0.3 \text{ eV} \lesssim |\mu_{Al}| \lesssim 0.5 \text{ eV}$  interrupted Al chains with vacancy period five/six will be formed both along the terrace and groove sites. It is significant to note that for  $0 < |\mu_{Al}| \lesssim 0.3 \text{ eV}$ , continuous Al chains along the terrace sites assisted by the interrupted Al chain (with vacancy period five/six) along the groove sites can be formed. We note that the experimentally observed  $1 \times 6$  surface pattern for Al/Si(211) corresponds to one of the favorable structures presented here within the  $0 \text{ eV} < |\mu_{Al}| \lesssim 0.5 \text{ eV}$ . A novel finding is that an uninterrupted Al chain may be formed on Si(211) unlike the case of Ga and In on Si(211). Furthermore, the Al covered Si(211) surface may be metallic or semiconducting in nature depending on the experimental conditions, while the Ga covered Si(211) surface is only semiconducting in nature below 1 ML coverage. One would expect that since Al ( $3s^23p^1$ ) and Ga ( $4s^24p^1$ ) belong to the same column of the periodic table, they should manifest similar physical and chemical properties. This is certainly true at a gross level but their behavior at surfaces can be very different due to differences in lattice constants but more significantly due to major differences in their cohesive energies. It should be noted that cohesive energy of Al ( $\sim 4 \text{ eV}$ ) is at least  $\sim 0.5 \text{ eV}$  larger (more strongly bound by this amount) than for Ga. When it comes to binding on surfaces of other materials, there is a competition between cohesion and bonding and hence it is not surprising that Al and Ga may stabilize in different configurations on Si(211). The STM experiments on the Al/Si(211) system will be helpful in revealing both the continuous and interrupted Al wire structures.

- 
- <sup>1</sup> J. N. Cria, A. Kirakosian, K. N. Altmann, C. Bromberger, S. C. Erwin, J. L. McChesney, J. -L. Lin, and F. J. Himpsel, *Phys. Rev. Lett.* **90**, 176805 (2003).
  - <sup>2</sup> J. N. Crain, J. L. McChesney, Fan Zheng, M. C. Gallagher, P. C. Snijders, M. Bissen, C. Gundelach, S. C. Erwin, and F. J. Himpsel, *Phys. Rev B* **69**, 125401 (2004).
  - <sup>3</sup> I. P. Batra, *Phys. Rev. Lett.* **63**, 1704 (1989).
  - <sup>4</sup> B. C. Gupta and I. P. Batra, *Phys. Rev. B* **69**, 165322 (2004).
  - <sup>5</sup> *Advances in Scanning Probe Microscopy*, edited by T. Sakurai and Y. Watanabe (Springer-Verlag, Berlin, 1989).
  - <sup>6</sup> S. Watanabe, Y. Ono, T. Hashizume, and Y. Wada, *Phys. Rev. B* **54**, R17308 (1996).
  - <sup>7</sup> B. C. Gupta and I. P. Batra, *Phys. Rev. B* **71**, 165429 (2005).
  - <sup>8</sup> D. J. Chadi, *Phys. Rev. B* **29**, 785 (1984).
  - <sup>9</sup> R. Kaplan, *Surf. Sci.* **116**, 104 (1982).
  - <sup>10</sup> J. E. Yater, A. Shih, and Y. U. Idzerda, *Phys. Rev. B* **51**, R7365 (1995).
  - <sup>11</sup> O. J. Glemblocki and S. M. Prokes, *Appl. Phys. Lett.* **71**, 2355 (1997).
  - <sup>12</sup> A. A. Baski, S. C. Erwin, and L. J. Whitman, *Surf. Sci. Letters*, **423** L265 (1999).
  - <sup>13</sup> C. Gonzalez, P. C. Snijders, J. Ortega, R. Perez, F. Flores, S. Rogge, and H. H. Weitering, *Phys. Rev. Lett.* **93**, 126106 (2004).
  - <sup>14</sup> Z. Gai, R. G. Zhao, W. S. Yang, and T. Sakuri, *Phys. Rev. B* **61**, 9928 (2000).
  - <sup>15</sup> X. Wang and W. H. Weinberg, *Surf. Sci.* **314**, 71 (1994).
  - <sup>16</sup> T. Berghaus, A. Brodee, H. Neddermeyer and S. Tosch, *Surf. Sci.* **184**, 273 (1987).
  - <sup>17</sup> P. Sen, I. P. Batra, S. Sivananthan, C. H. Grein, N. K. Dhar and S. Ciraci, *Phys. Rev. B* **68** 045314 (2003).
  - <sup>18</sup> A. A. Baski, S. C. Erwin, and L. J. Whitman, *Surf. Sci.*, **392** 69 (1997).
  - <sup>19</sup> A. A. Baski and L. J. Whitman, *Phys. Rev. Lett.* **74** 956 (1995).
  - <sup>20</sup> S. Mankefors, *Surf. Sci.* **443**, 99 (1999).
  - <sup>21</sup> D. Vanderbilt, *Phys. Rev. B* **41**, 7892 (1990); G. Kresse and J. Hafner, *J. Phys.: Condens. Matter* **6**, 8245 (1994).
  - <sup>22</sup> J. P. Perdew and Y. Wang, *Phys. Rev. B* **46**, 6671 (1992).
  - <sup>23</sup> G. Kresse and J. Hafner, *Phys. Rev. B* **47**, R558 (1993); G. Kresse and J. Furtmüller. *Phys. Rev. B* **54**, 11169 (1996).
  - <sup>24</sup> S. C. Erwin, A. A. Baski, L. J. Whitman and R. E. Rudd, *Phys. Rev. Lett.* **83**, 1818 (1999).